

JET disruption simulations

H. Strauss¹, R. Paccagnella², J. Breslau³, E. Joffrin⁴, V. Riccardo⁵, I. Lupelli⁵, M. Baruzzo²

and JET Contributors*

¹ *HRS Fusion, West Orange NJ, USA*

² *Consorzio RFX and Istituto Gas Ionizzati del C.N.R., Padua, Italy*

³ *Princeton Plasma Physics Laboratory, Princeton, NJ, USA*

⁴ *IRFM, CEA centre de Cadarache, 13108 Saint-Paul-lez-Durance*

⁵ *EURATOM/UKAEA Fusion Association, Culham Science Centre, OX14 3DB, UK*

EUROfusion Consortium, JET, Culham Science Centre, Abingdon, OX14 3DB, UK

Introduction

The JET tokamak is a main source of information about the possible effects of disruptions [1, 2, 3] in ITER. JET measurements indicate large forces will be generated on conducting structures surrounding the plasma. It was also found in JET that the halo current, the plasma current asymmetry, and hence the wall force, rotates during disruptions. This is potentially important if the force oscillations are resonant with the mechanical response of the external structure. Recently JET disruption simulations using the M3D (3D MHD) code [4] were carried out, initialized with an EFIT equilibrium reconstruction of disruption shot 72926 [1, 2] at time at time 66998ms. The simulations are carried out much further in time than previously [5, 6, 7].

The simulations have several features in common with experiment. There is a rapid thermal quench (TQ), followed by a slower vertical displacement event (VDE). During the TQ and the VDE, there is an asymmetric force on the wall surrounding the plasma, whose magnitude is consistent with experiment. Most of the force impulse occurs during the VDE phase. During this phase toroidal momentum is generated, which causes rotation of the direction of the asymmetric wall force [6, 7]. During the VDE, the toroidal current and the toroidal magnetic flux vary toroidally, effects which are observed experimentally [3]. The resistive wall time τ_{wall} is varied in the simulations, and it is found that the wall force depends on τ_{wall} , as in previous work [5]. If there is vertical control to suppress the VDE, the wall force is strongly mitigated.

The JET shot had magnetic field $B = 2T$, and a carbon wall. It differed from the simulations in several respects. The plasma resistivity, measured by the Lundquist number S , and the wall resistivity measured by $S_{wall} = \tau_{wall}/\tau_A$ were lower than in the experiment, where τ_{wall} is the resistive wall penetration time, and $\tau_A = R/v_A$ is the Alfvén time, with major radius R and Alfvén speed v_A . In all the simulations, the Lundquist number is $S = 10^6$, and $400 \leq S_{wall} \leq 1300$. The current in the simulations was held constant until the plasma reached the wall, when

the simulation was terminated. The JET wall time is 5ms [8] and taking the JET Alfvén time as $\tau_A \approx 7 \times 10^{-7}$ s, then $S_{wall} \approx 7 \times 10^3$.

The equilibrium reconstruction shows that $q \approx 0.8$ at the magnetic axis just before the disruption. The equilibrium is unstable both to an internal kink mode and a VDE. The large scale kink mode destabilizes or drives other modes, causing a turbulent state and producing the TQ, which occurs on a rapid timescale. This is followed by the VDE which evolves on the slow resistive wall penetration timescale. During the VDE, a (2, 1) mode becomes unstable. The interaction

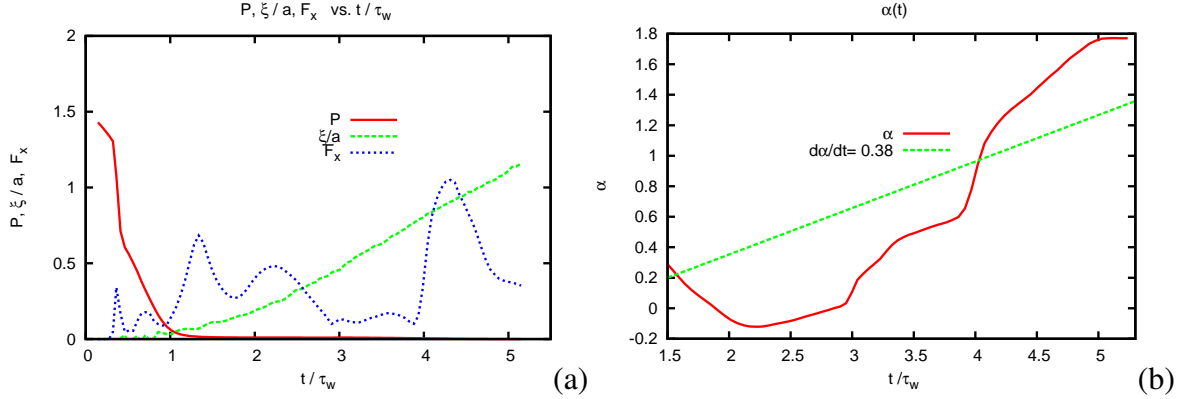


Figure 1: (a) Time history of the total pressure P , vertical displacement ξ/a , and (b) force angle as a function of time.

of the (2, 1) mode and the (1, 0) VDE causes asymmetric wall force to be produced [5].

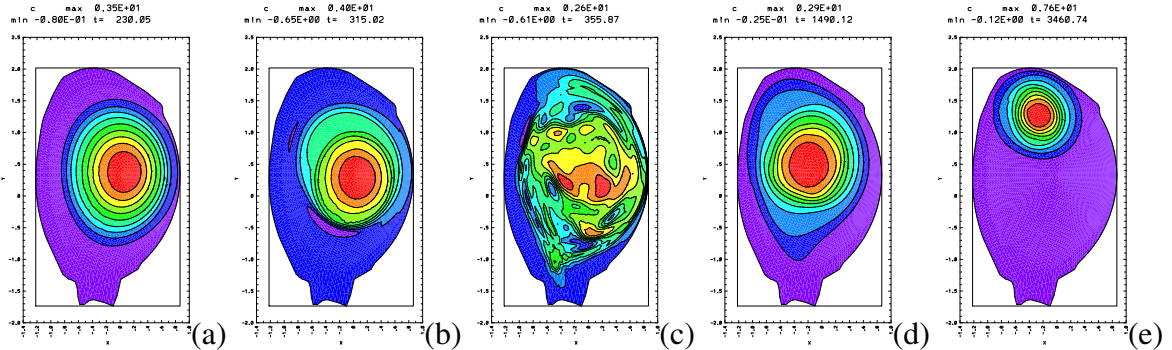


Figure 2: Current density contours for the run of Fig.1 in a plane of constant toroidal angle at different times: (a) initial state, (b) internal (1,1) kink instability, at time $t = .47\tau_{wall}$, (c) turbulent state at time of TQ, $t = .53\tau_{wall}$, (d) VDE with (2,1) mode, at $t = 1.9\tau_{wall}$, (e) scrape off of flux and (2,1) mode at $t = 4.3\tau_{wall}$.

Fig.1(a) shows the time evolution of the normalized pressure P integrated over the plasma volume. The pressure drops rapidly to about half its initial value at time $t \approx 0.5\tau_{wall}$, in about

$10^2 \tau_A$. The resistive wall time is $\tau_{wall} = S_{wall} \tau_A$, which in this simulation is $S_{wall} = 800$. Fig.1(a) also shows the time development of the VDE displacement ξ , normalized to the minor radius a . When ξ/a approaches unity, the plasma and magnetic flux are scraped off at the wall. Fig.1(a) also shows the asymmetric force or sideways F_x [6, 7]. The sideways force has several temporal peaks during the VDE, with maximum value $F_x \approx 1MN$.

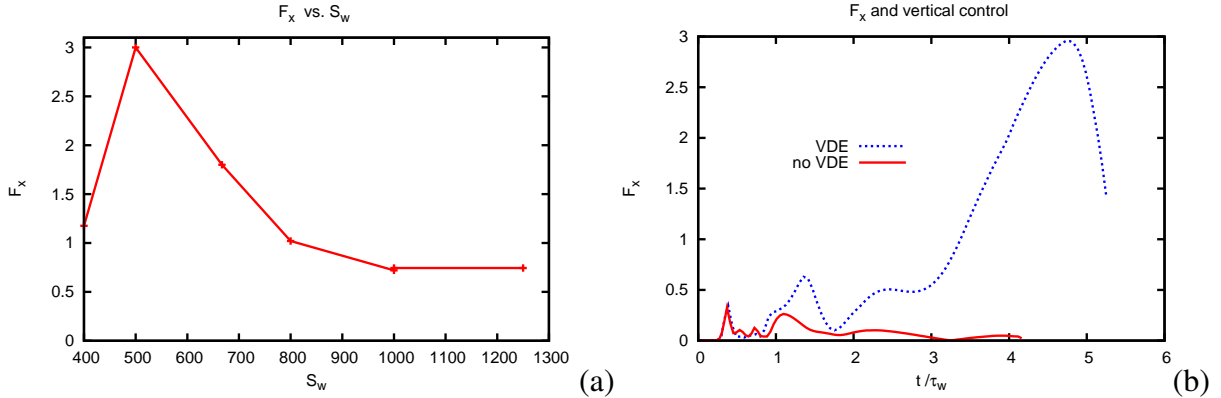


Figure 3: *Mitigating effects: (a) Maximum force amplitude as a function of S_{wall} . (b) Time history of the asymmetric wall force F_x , with and without vertical control.*

The (1, 1) mode is seen to reach large amplitude in Fig.2(b). The TQ then follows, at Fig.2(c) the current contours have broken up, suggesting a breakup of the magnetic surfaces. In Fig.2(d), the current surfaces are restored, with a large vertical displacement, and (2, 1) perturbation. In Fig.2(e), the (1, 0) displacement $\xi \approx a$.

Wall force rotation

The sideways force rotates during the VDE phase. The force rotation was measured from the force angle $\alpha = (2\pi)^{-1} \tan^{-1} F_{xy}/F_{xx}$, where F_{xx}, F_{xy} are the \hat{x} and \hat{y} components of the toroidally varying wall force in the midplane. Fig.1(b) shows the time history of α , for the same case as in Fig.1(a), and $d\alpha/dt \approx 3.8 \times 10^{-4} \tau_A^{-1} \approx 540Hz$. The frequency is comparable to the peak spatially averaged toroidal velocity V_ϕ [7]. These frequencies are not sensitive to the value of S_{wall} . In the experiment the frequency was $f = 280Hz$ [1, 2].

Mitigating effects of resistive wall time and vertical control

The value of S_{wall} was varied in order to examine its effect on the force and rotation rate. The maximum force varied substantially, while the rotation was only weakly dependent on S_{wall} . Fig.3(a) shows how the peak force depends on S_{wall} . According to [5], the sideways force peaks when the (2, 1) growth rate $\gamma \tau_w \sim 1$. For a tearing mode, γ depends on S , hence Fig.3(a) may depend on S as well as S_{wall} . The force asymptotes to a constant, lower value for large S_{wall} ,

which depends on the (1, 1) mode, as shown in [5]. The wall force in the figures is scaled so that $F_x = 1.0$ is [5] 1MN. The maximum force, with $S_{wall} = 500$, is 3MN.

In Fig.3(b) are shown the wall force as a function of time in two cases with $S_{wall} = 500$. In the first case, the maximum wall force corresponds to the peak value in Fig.3(a). In the second case, the VDE is suppressed by setting the time evolution of the toroidally averaged normal magnetic field at the wall to zero, $\oint d\phi (\partial B_n / \partial t) = 0$, eliminating the interaction of the (2, 1) and (1, 0) modes and mitigating the wall force.

Toroidal flux and current asymmetry

In [3], the toroidal flux and current in JET were shown to vary toroidally during a disruption. Here the toroidal flux is $\Phi = \int B_\phi d^2x$, the toroidal current is $I = \int J_\phi d^2x$, the asymmetric toroidal flux is $\Delta\Phi = (2\pi)^{-1/2} [\oint \tilde{\Phi}^2 d\phi]^{1/2}$, and the asymmetric toroidal current is $\Delta I = (2\pi)^{-1/2} [\oint \tilde{I}^2 d\phi]^{1/2}$, where $\tilde{\Phi} = \Phi - \oint \Phi d\phi / 2\pi$. The time evolution of $\Delta\Phi, \Delta I$ are shown in Fig.4 for $S_{wall} = 800$. The toroidal variation of toroidal current and toroidal flux follow from $\nabla \cdot \mathbf{B} = 0$, and $\nabla \cdot \mathbf{J} = 0$, which have the integral form, where dl is the wall length element, $\partial\Phi/\partial\phi = -\oint B_n R dl$, $\partial I/\partial\phi = -\oint J_n R dl$. Suppose $J_\phi = \lambda B_\phi$, then $\partial I/\partial\phi = \lambda \partial\Phi/\partial\phi$. Taking $\lambda \approx I/\Phi$ gives $\Delta\Phi/\Phi \approx \Delta I/I$, which is consistent with Fig.4.

*See the Appendix of F. Romanelli et al., Proceedings of the 25th IAEA Fusion Energy Conference 2014, Saint Petersburg, Russia

Acknowledgement: research supported by USDOE and within the framework of the EUROfusion Consortium, and has received funding from the Euratom research and training programme 2014-2018 under grant agreement No 633053. The views and opinions expressed herein do not necessarily reflect those of the European Commission.

References

- [1] S.N. Gerasimov, T.C. Hender, J. Morris, *et al.*, Nucl. Fusion **54** 073009 (2014).
- [2] V. Riccardo, G. Arnoux, P. Cahyna, *et al.*, Plasma Physics and Controlled Fusion **52** 124018 (2010).
- [3] S. N. Gerasimov, P. Abreu, M. Baruzzo, *et al.*, Nucl. Fusion **55** 113006 (2015).
- [4] W. Park, E. Belova, G. Y. Fu, X. Tang, H. R. Strauss, L. E. Sugiyama, Phys. Plasmas **6** (1999) 1796 (1999).
- [5] H. Strauss, R. Paccagnella, J. Breslau, L. Sugiyama, S. Jardin, Nucl. Fusion **53**, 073018 (2013).
- [6] H. R. Strauss, L. Sugiyama, R. Paccagnella, J. Breslau, S. Jardin, Nuclear Fusion **54**, 043017 (2014).
- [7] H. Strauss, Phys. Plasmas **22**, 082509 (2015)
- [8] V. Riccardo, T. C. Hender, P. J. Lomas, *et al.* Plasma Phys. Control. Fusion **46**, 925 (2004).

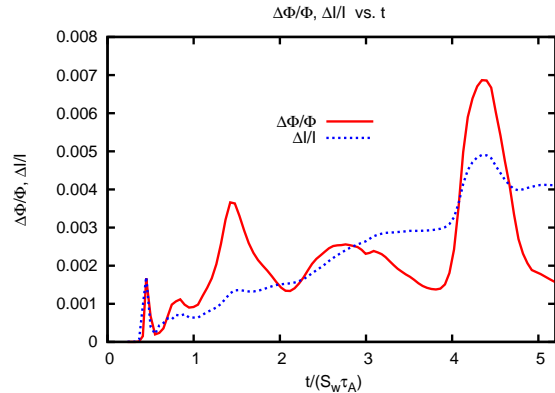


Figure 4: Time history of the toroidal variation of toroidal current $\Delta I/I$ and of toroidal magnetic flux $\Delta\Phi/\Phi$.